Assessing the Contribution of the Arctic Weather Satellite 325.15 GHz Channels to Improve Observation of Precipitation Events

Andrea Camplani; Paolo Sanò; Daniele Casella; Leo Pio D'Adderio;
Stefano Sebastianelli; Daniele D'Armiento; Laura Soncin; Giulia Panegrossi
National Research Council of Italy, Institute of Atmospheric Sciences and Climate, Rome, Italy

1. Introduction

- satellite observations are fundamental to study precipitation events, especially in areas where in-situ instruments are almost absent (e. g., oceanic basins and polar areas)
- VIS/IR sensors from geostationary satellite do not provide information about precipitation
- microwave wavelengths are directly responsive to hydrometeors in precipitating clouds
- satellite radar observations are limited in spatial coverage
- passive microwave (PMW) sensors ensure an high spatial and temporal coverage

2. Arctic Weather Satellite

AWS

- launched in August 2024
- polar-orbiting satellite
- forerunner of the EUMETSAT Polar System-Sterna (EPS-Sterna) mission, a constellation of small polar-orbiting satellites - from 2029
- carrying Microwave Radiometer (MWR)

MWR

- cross-track scanning radiometer
- 19 channels, frequency range 50–325 GHz, 4 receiver chains – different footprints for each channels group (*Eriksson et al., 2025*)
- 4 new channels in the 325.15 GHz water vapor absorption band
- coupled channels at 183.31 and 325.15 GHz (*Camplani et al., 2024*)
  - very similar weighting functions in clear sky (see Figure on the right)
  - very different scattering response to the presence of cloud ice
- data available from March 2025

AWS-MWR			
Freq. (GHz)	n ch	Pol.	Footprint (km)
50.3	8	QV	< 40
89	1	QV	< 20
165.5	1	QV	< 10
183.31	5	QV	< 10
325.15	**4**	**QV**	**< 10**

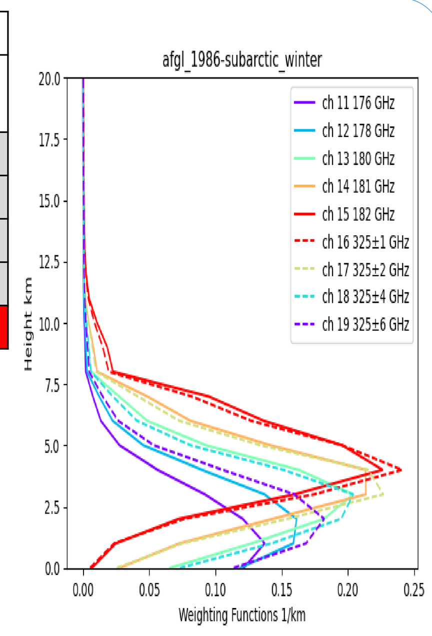

3. Reference Products

The analysis has been carried out by comparing the PMW brightness temperature (TB) measurements with nearly coincident spaceborne radar measurements

- the Dual-Frequency Precipitation Radar (DPR) onboard the GPM – Core observatory (GPM-CO) is the reference for rainfall
  - KuPR product (*Iguchi et al., 2010)*
  - CORRA product (*Olson et al., 2022)*
- the Cloud Precipitation Radar (CPR) and Atmospheric Lidar (ATLID) onboard EarthCare (EC) are the reference for the snowfall
  - ACM-CAP product (*Mason et al., 2023*)

4. Rainfall Event: Hurricane Melissa, 2025/10/30

- 2025/10/21-31
- Caribbean Sea
- it reached the Category 5 of the Saffir-Simpson Scale
- pressure down to 892 hPa
- maximum sustained wind at 300 km h^{-1}

Case Study

- 2025/10/30, at around 3:00 UTC
- north of Cuba (hurricane eye at 24 ° N, 74 °W)
- hurricane observed in its mature phase
- Category 1 of the Saffir - Simpson Scale
- coincident overpass between
  - AWS (2:51-2:54 UTC)
  - GPM-CO (2:56-2:59 UTC)
- time span between observations ≈ 5 min

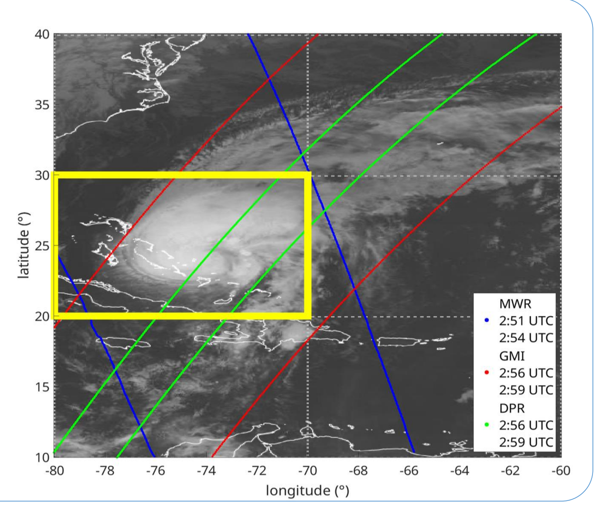

4.1 DPR Observations

KuPR Product (a,b,c)

- eastern part of the cyclone
- eye at 24 ° N, 74 ° W
- 3 high reflectivity rainbands
- 2 areas characterized by high values of storm top height (STH>10 km)
- 2 bands classified as convective clouds around the eye

Precipitation Estimates from CORRA product (d)

- Total Precipitation Rate (TPR, precipitation at the ground level) > 150 mm h^{-1}

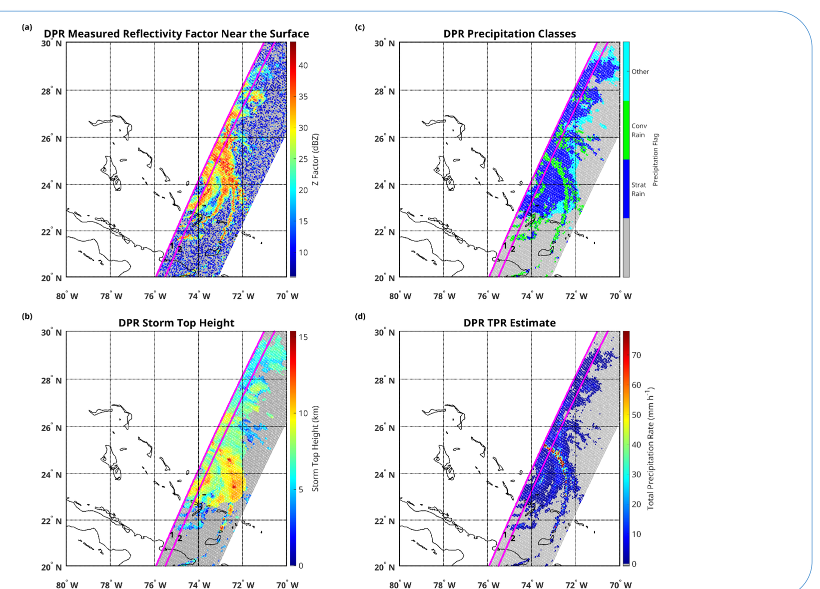

4.2 AWS-MWR Observations

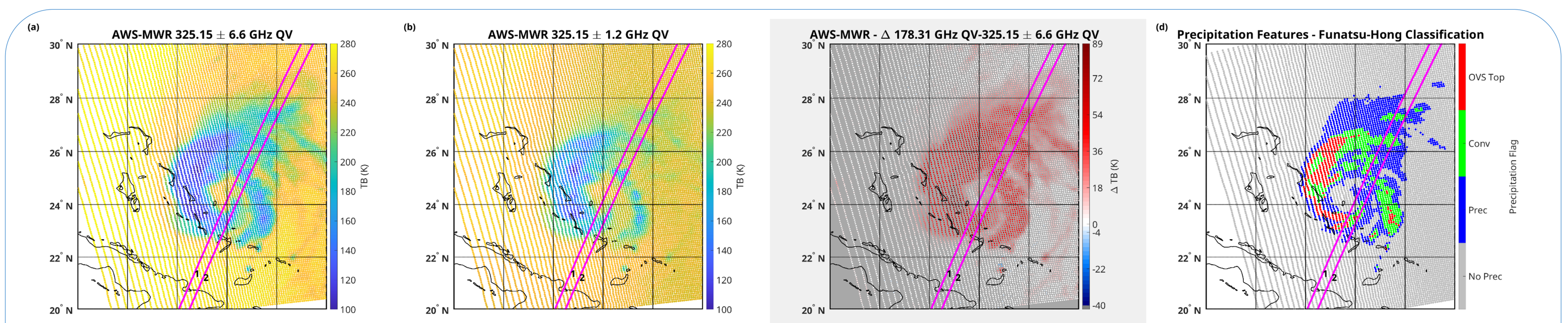

- both in 325.15 GHz maps (a,b) and in ΔTB 183.31-325.15 GHz TB map (c) a clear and intense cloud signal is visible -TB cooling in (a,b), ΔTB > 0 K in (c)
- The signal tends to saturate for the 325.15 GHz external channel (a) and the ΔTB between external channels (c)
- for the 325.15 GHz internal channel (c) maps areas where the scattering effect is visible are thinner, and higher variability in TB values is observed in areas where the TB depression at 325.15±6.6 GHz is saturated

Funatsu-Hong Classification

- a classification of the precipitation features based on *Funatsu et al., 2007* and *Hong et al., 2005* that exploit 183.31 GHz channels and identifies 3 classes (precipitation, convective clouds, overshooting tops)
- eye is identified in correspondence with DPR
- convective cloud areas are larger than those identified by DPR
- overshooting tops areas roughly correspond to DPR convection areas

4.3 AWS-MWR-DPR Comparison along Cross Sections

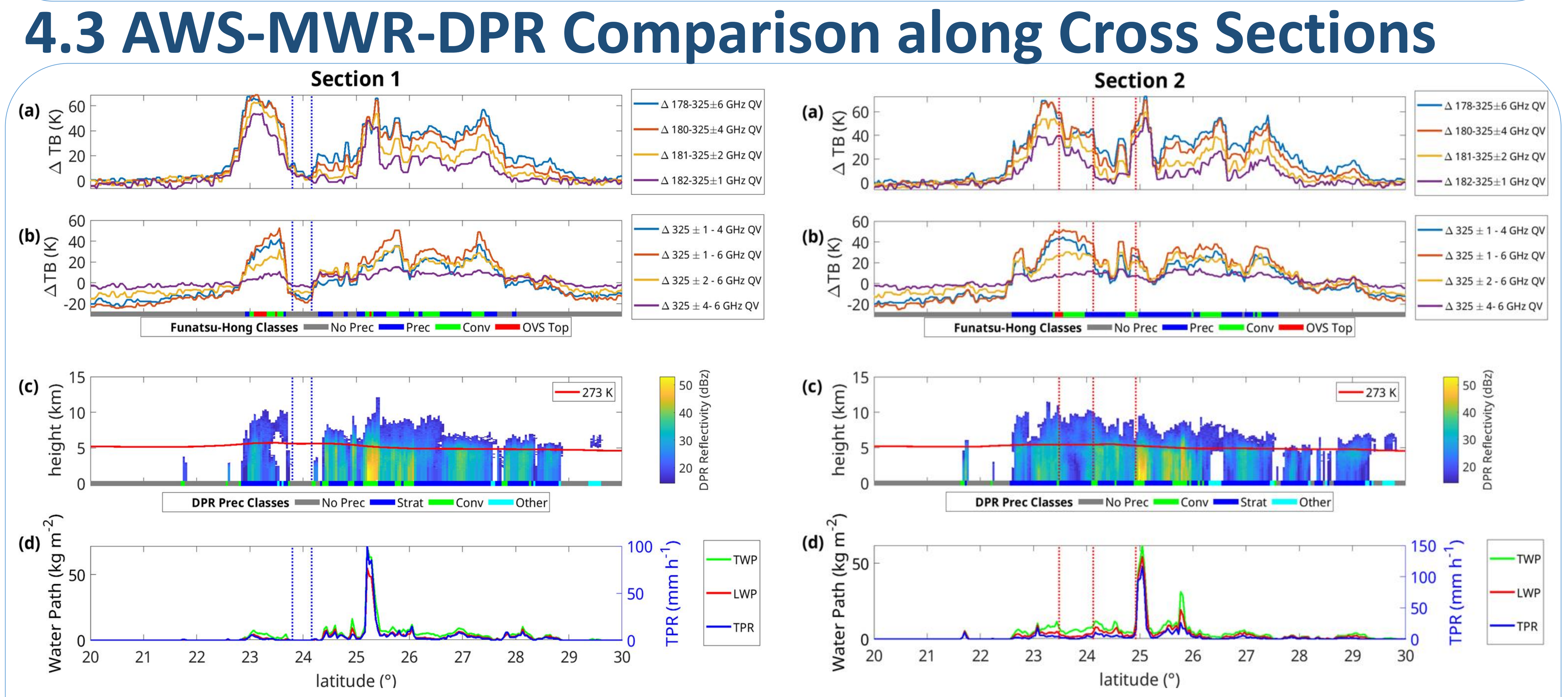

- in (a) and (b) the max ΔTBs around the eye area (blue dotted lines) are similar, while Total Water Path (TWP) and TPR values in (d) are different
- the eye region - identified by DPR (blue dotted lines) - is narrower than the region identified by Funatsu-Hong classes - along x axis in (b)
- in (b) a very good correspondence between the eye area and areas where Δ325 1-6 (b, orange line) is < -10 K & Δ325 1-6<Δ325 1-4,(b, blue line)

in (a)

- Δ183-325≈0 K in clear-sky areas, Δ183-325 > 0 K in cloudy areas
- Δ183-325 between the external channels (blue line) are generally > than Δ183-325 between the internal channels (e.g., orange line) in cloudy conditions, except from where DPR identified convective clouds - along x-axis in (c) (e. g., red dotted lines)

5. Snowfall Event: Arctic Ocean, 2026/02/24-25

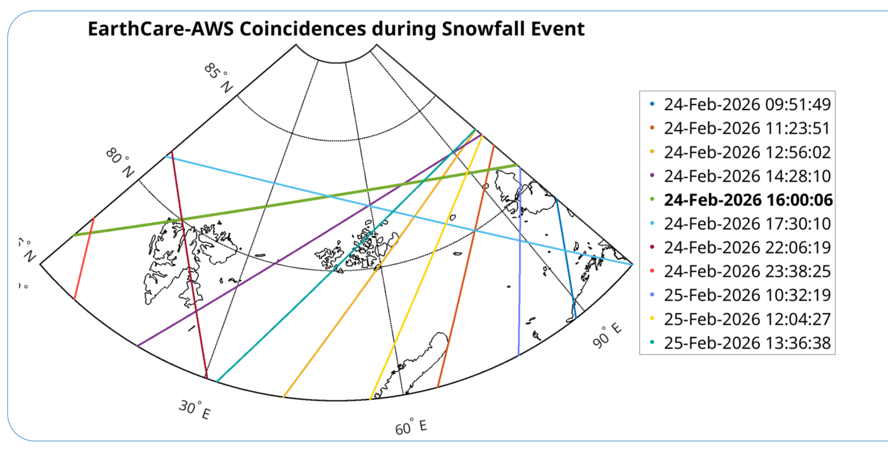

Snowfall event linked to a Warm Air Intrusion event

- 11 AWS-EarthCare coincident observations
- typical winter arctic environmental conditions (TPW< 10 mm, T_{2m}<273 K)
- both sea ice and open water as background surface

5.1 AWS-MWR-EarthCare Comparison

- ACM-CAP (d,f) detects presence of cloud ice – with two maxima around 10°W and 30°W (blue line, f)
- ACM-CAP (d,f) detects the presence of supercooled liquid water (SLW)
- transition from relatively warm and humid conditions very cold and dry from west to east (e)
- the 50.3 GHz TBs (a, blue line) raise sharply in the center of the considered areas – sea ice/open water interface
- correspondence between 89 GHz TBs increase (a, orange line) and presence of SLW (d, magenta points) on the western region - open water as background
- the Δ 183.31 GHz TBs (b) tend to increase as the environmental conditions (e) becomes colder and drier
- strong correspondence between high Ice Water Path (IWP) values (f, blue line) and positive values of the differences between the 183-325 GHz coupled channels (Δ 178-325±6 GHz TB, c, blue line)

- 2025/02/24, at around 16:00 UTC
- EC overpass represented by the green line in the map in Box 5
- coincident overpass between
  - EC (15:56-16:03 UTC)
  - GPM-CO (15:59-16:06 UTC)
- time span between observations ≈ 5 min

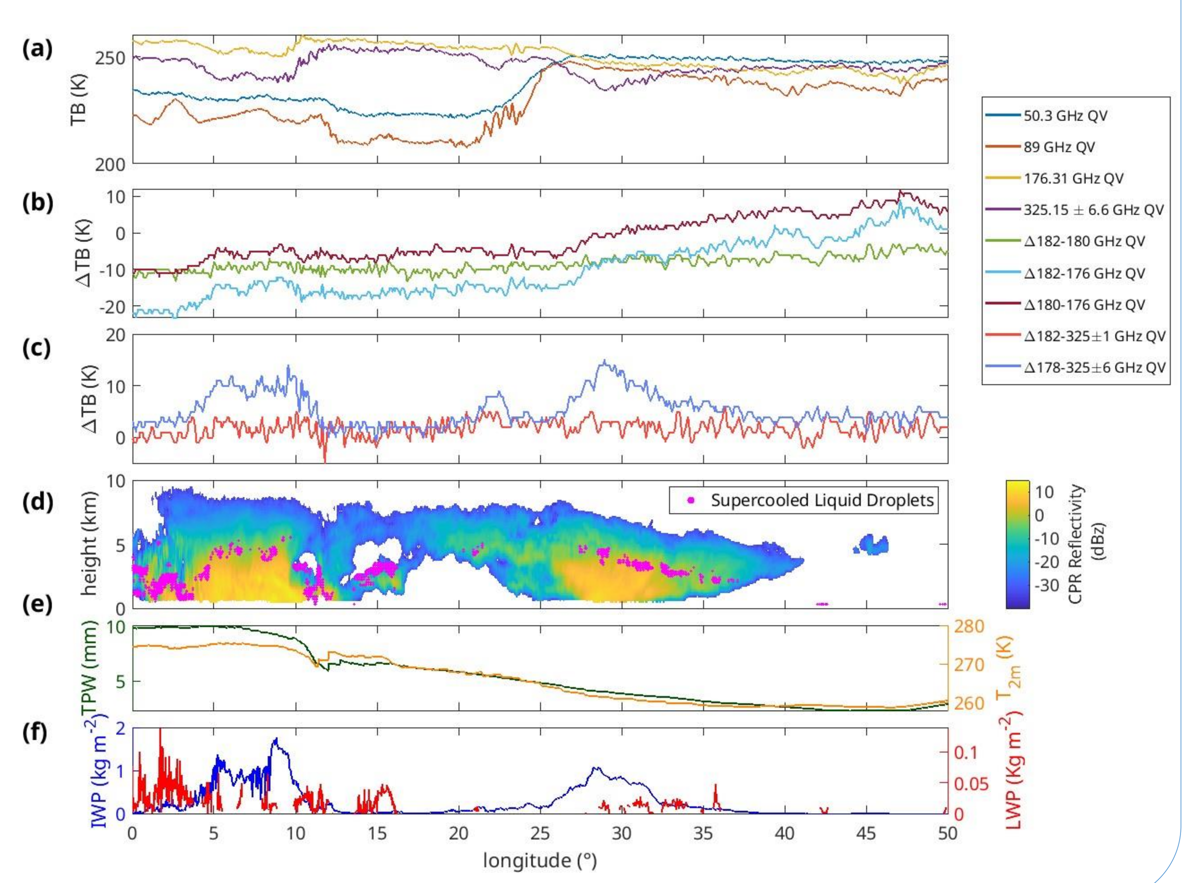

5.2 AWS-MWR Observations

- the 50.3 GHz map shows a clear raise of the TB corresponding to the open water/sea ice boundary
- The 176.31 GHz map (b) shows a very weak scattering (TB cooling) signal in correspondence with the snowfall event at 10°W along the EC track and no sensitivity to the snowfall event at 30°W
- The 325.15 ±6.6 GHz map (c) shows a clear scattering signal in correspondence with both snowfall events
- the Δ 178.31-325.15±6.6 GHz TB map (d) shows strong sensitivity (ΔTB up to 17 K) in correspondence with both snowfall events. The noisy signal is likely due to geolocation mismatch between the 183.31 GHz and 325.15 GHz footprints

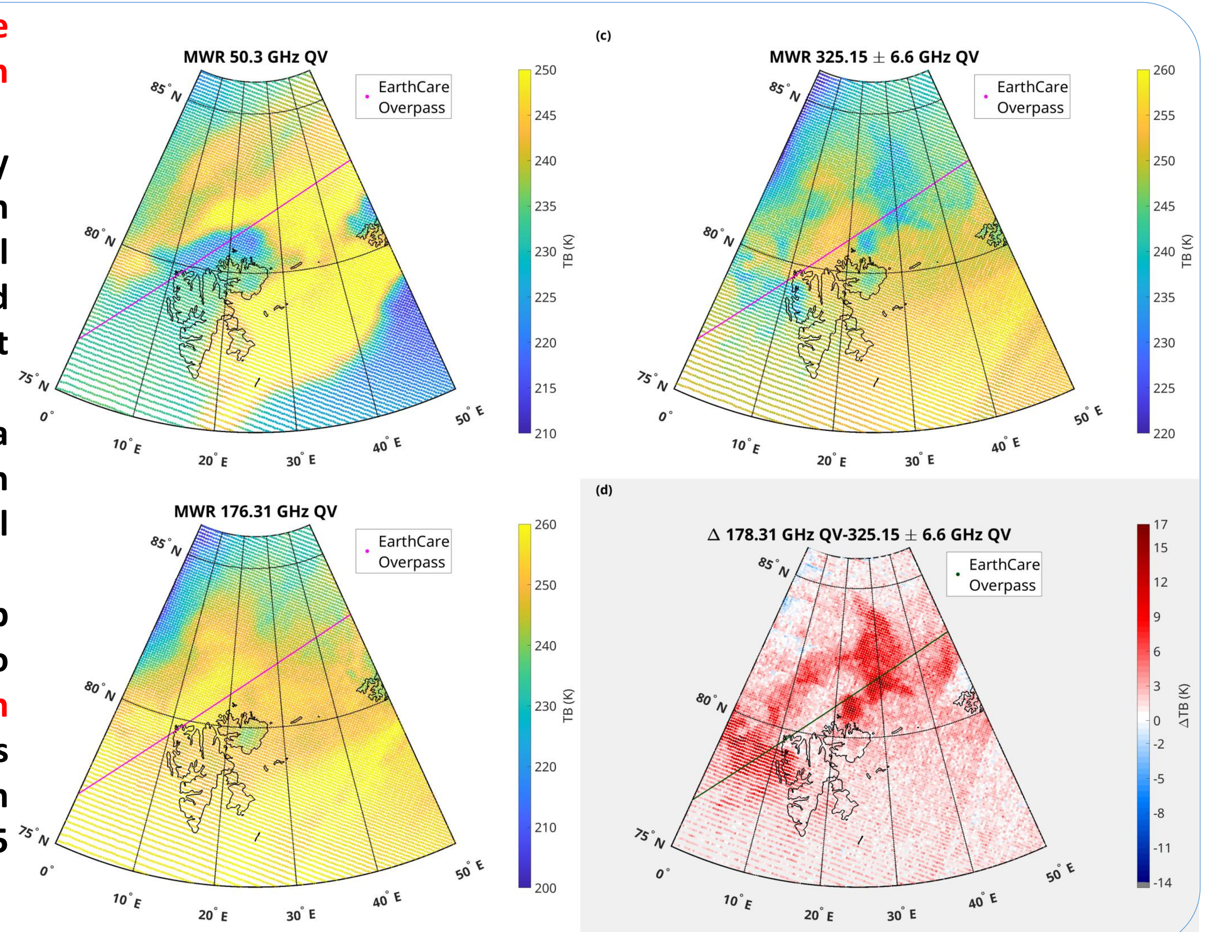

5.3 Analysis of the ΔTB signal over All Overpasses

- the Δ 178-325±6 GHz increases as the IWP increase (a), in particular for IWP > 0.1 kg m^{-2}
- the Δ 183.31 GHz values show no significant correlation with the IWP (a)
- significant anti-correlation between the ΔTB 182.31-176.31 GHz values and Total Precipitable Water (TPW) (b)
- weak correlation between the Δ 178.31-325.15±6.6 GHz TB and TPW – due to the increase of IWP in moist conditions (b)

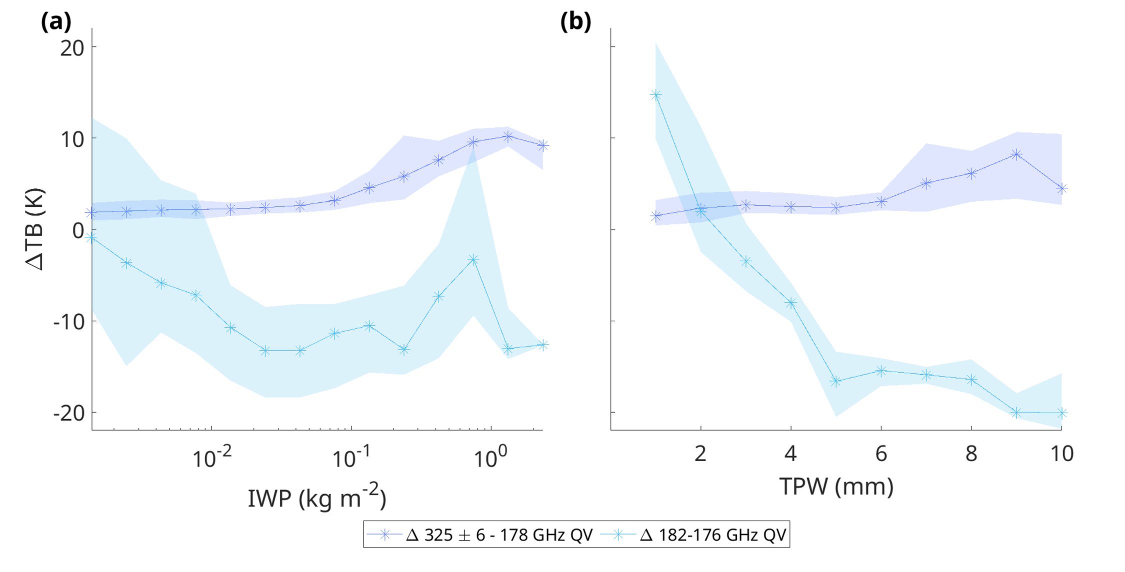

6. Conclusions and Future Developments

- AWS-MWR observations are very effective to characterize both tropical rainfall and snowfall events
- For what concerns tropical cyclones
  - AWS-MWR 325 GHz channel TB signal tends to saturate in correspondence with high precipitation values…
  - …but can be useful to characterize some features of the precipitation structure in better agreement with DPR with respect to 183 GHz channels TBs only, such as the definition of cloud-free area and the identification of convective systems
- For what concerns snowfall
  - the 325 GHz channels show strong sensitivity to the weak scattering signal of snowfall in polar regions
  - the Δ 178.31-325.15±6.6 GHz seems to be an very good proxy for IWP estimation also for very low IWP – down to 0.1 kg m^{-2}
  - the 89 GHz show strong sensitivity to SLW over open water
- For the future
  - reduction of the noise in the ΔTBs - testing new co-location methodologies
  - creation of coincidence dataset from AWS-DPR and AWS-EC, to be used in retrieval algorithm training

7. References

Eriksson, P., et al. "The Arctic Weather Satellite radiometer." Atmospheric Measurement Techniques 18.18 (2025): 4709-4729, https://doi.org/10.5194/amt-18-4709-2025, 2025

Camplani, A., et al. "Arctic Weather Satellite sensitivity to supercooled liquid water in snowfall conditions." Remote Sensing 16.22 (2024): 4164, https://doi.org/10.3390/rs16224164

Iguchi, T., et al. "GPM/DPR level-2 algorithm theoretical basis document." NASA Goddard Space Flight Center 750 (2010), https://gpm.nasa.gov/sites/default/files/2024-09/ATBD_DPR_L2.pdf.

Olson, W. S., et al. "GPM Combined Radar-Radiometer Precipitation Algorithm Theoretical Basis Document (Version 7)." NASA: Washington, DC, USA (2022), https://gpm.nasa.gov/sites/default/files/2023-01/Combined_algorithm_ATBD.V07_0.pdf

Mason, S. L., et al. "A unified synergistic retrieval of clouds, aerosols, and precipitation from EarthCARE: the ACM-CAP product." Atmospheric Measurement Techniques 16.13 (2023): 3459-3486, https://doi.org/10.5194/amt-16-3459-2023

Kelly .A., et al. "Hurricane Melissa (AL132025) 21–31 October 2025", National Hurricane Center (2026), https://www.nhc.noaa.gov/data/tcr/AL132025_Melissa.pdf

Funatsu, B., et al. "Potential of Advanced Microwave Sounding Unit to identify precipitating systems and associated upper-level features in the Mediterranean region: Case studies." Journal of Geophysical Research: Atmospheres 112.D17 (2007), https://doi.org/10.1029/2006JD008297

Hong, G., et al. "Detection of tropical deep convective clouds from AMSU-B water vapor channels measurements." Journal of Geophysical Research: Atmospheres 110.D5 (2005), https://doi.org/10.1029/2004JD004949

SHARING IS ENCOURAGED

Contact

Andrea Camplani
Mail: andreacamplani@cnr.it

Acknowledgements

This work has been supported by EUMETSAT HSAF CDOP-4 and by EUMETSAT Project SLALOM-AWS Contract EUM/CO/26/4600002995/VBa